Received: 26 November 2019 | Revised: 26 November 2019 | Accepted: 12 December 2019

DOI: 10.1111/ijac.13456

ORIGINAL ARTICLE

International Journal of Applied Ceramic TECHNOLOGY

Preparation, characterization, and physical properties of lightweight ceramics by using sewage sludge ash

Asmaa A. Negm[1] | **Tarek Y. Elrasasi**[2] | **Hanem A. Khoder**[2] | **Fatma M. Metawe**[1] | **Mabrouk K. El-Mansy**[2]

[1]Basic Science Department, Faculty of Engineering at Shoubra, Benha University, Cairo, Egypt

[2]Physics Department, Faculty of Science, Benha University, Benha, Egypt

Correspondence
Asmaa A. Negm, Basic Science Department, Faculty of Engineering at Shoubra, Benha University, Cairo, Egypt.
Email: asmaanegm@yahoo.com.

Abstract

In the present study, sewage sludge ash (SSA) was added to clay to prepare lightweight ceramics for sustainable construction materials. The characterization and the effect of different concentrations of SSA on the physical and mechanical properties of the samples were studied. The results showed that the organic matter in SSA facilitated the combustion process. SSA addition reduced the bulk density from (1.94 to 1.32 g/cm^3). Otherwise, the water absorption, the apparent porosity and the loss on ignition increased with the increase in SSA concentration. The addition of SSA lowered the compression strength but still within the standard range of the construction materials at concentration up to (30 wt.%). Furthermore, heavy metals are solidified inside the sintered samples, since Cu, Cd, Fe, Zn, Cr, Mn, Ni, and Pb, concentrations in the leachate met the range of Egyptian standard specification.

KEYWORDS

ceramic engineering, characterization, porous materials, waste disposal

1 | INTRODUCTION

At present, the processing of waste is one of the most important challenges in the waste management everywhere.[1] Increasing the growth of cities and industry resulted in a massive increase in the volume of wastewater over the world.[2] Furthermore, by using suitable handling methods, a considerable amount of materials and energy can be retrieved from waste.[1] Sewage sludge ash (SSA) is a kind of semisolid waste that is produced as a byproduct during the sewage treatment of the industrial or the municipal wastewater treatment plants (WTP). SSA encloses a great number of pollutants such as organic contaminants, heavy metals, and pathogenic microorganisms, which represent serious negative environmental impact.[3]

So far, there are three main methods for the disposing of SSA such as sea dumping, soil application, and landfilling.[4] These methods are accompanied by some problems and hence negative environmental impact.[5] Problems of landfilling result from the high moisture state and high content of volatile solids in the sludge.[2] On the other hand, sea dumping causes water pollution and toxicity of sea biology.[2,6] The heavy metals contained in SSA cause the problems of soil application.[2] So, there must be novel methods for the disposing of this type of waste.

The reusing of SSA with the addition to clay to produce lightweight ceramic products is economically and environmentally promising. It reduces the consumption of clay and saves traditional raw materials, also provides appropriate disposing of the water treatment plant sludge so minimize the negative impacts of WTP residues on the environment.[7,8] SSA belongs to the renewable pore-forming agent since it has high organic matter content.[2,9] The break down of these compounds during the firing step of ceramics lead to the creation of pores that decrease ceramics density.[9] Using SSA to produce ceramic products can cut down the cost of the additional energy.[2] Therefore, the objective of the current research is to use SSA (containing a large amount of organic matter) with clay to prepare lightweight ceramic having good physical properties for sustainable construction materials.

2 | EXPERIMENTAL PROCEDURE

2.1 | Sewage sludge and clay samples

The SSA used in this work was collected from the water treatment plant in Benha (Egypt). The obtained SSA was dried at 105°C for 4 hours and then crushed by mortar to pass 212 μm sieves. The used clay was obtained from the Egyptian deserts. The samples of clay were milled and sieved to 212 μm particles in order to get a uniform particle size. The particle size distribution of both clay and SSA powders was determined by analytical shaker sieve (AS 200 control-RETSCH). The two curves of clay and SSA show particle sizes between 20 and 200 μm as shown in Figure 1. It is also seen that the average particle size, d50, is 100 and 109 μm for clay and SSA respectively.

2.2 | Preparation of ceramic samples

Four different weight percentages of SSA to clay were evaluated: (0, 10, 20, 30, and 40 wt.%). The materials were finely mixed using a mixer with dropwise of water (15% by weight) to induce some plasticity since water content is a key factor that can influence the shaping and the drying of the final product.[9,10] The mixtures were molded by cylindrical steel die with a diameter of 14.5 mm and a height of 17 mm by uniaxial pressing at a pressure of 105 MPa. An example of the green prepared samples is shown in Figure 2.

Green prepared samples were left at room temperature for 24 hours, followed by an oven drying at 105°C for another one hour so that the weight was maintained constant. After drying, samples were transferred to a laboratory electric furnace for sintering. Heating followed a system of gradual increase in temperature to avoid cracking since it takes 90 minutes until it reaches 600°C at which it is left for 1 hour then rises to the maximum temperature of 800°C and remains for 30 minutes. Finally, the prepared samples were left to cool down gradually. An example of the sintered sample is shown in Figure 3.

2.3 | Characterization

As the major properties of the ceramic materials are connected to their mineralogical composition, the raw materials and the prepared samples were analyzed by X-ray diffraction (XRD) with a Philips X-ray diffractometer using monochromatized CuKα1 radiation of wavelength 1.54056 Å from a fixed source operated at 45 kV and 9 mA, and the scanning electron microscope (SEM), Model Quanta 250 Field Emission Gun attached with EDX Unit (energy dispersive X-ray analyses), with accelerating voltage 30 kV. The differential thermal analysis (DTA) and thermo gravimetric analysis (TGA) using (STA 504) was used to investigate the thermal behavior during sintering in flowing nitrogen atmosphere at a heating rate 20°C/min in the range between room temperature and 900°C to obtain mass decomposition and phases transformation.

2.4 | Physical properties

Some physical parameters were measured on clay/SSA samples. These parameters include; bulk density (*B*), apparent porosity (*P*), water absorption (*A*), loss on ignition (LOI),

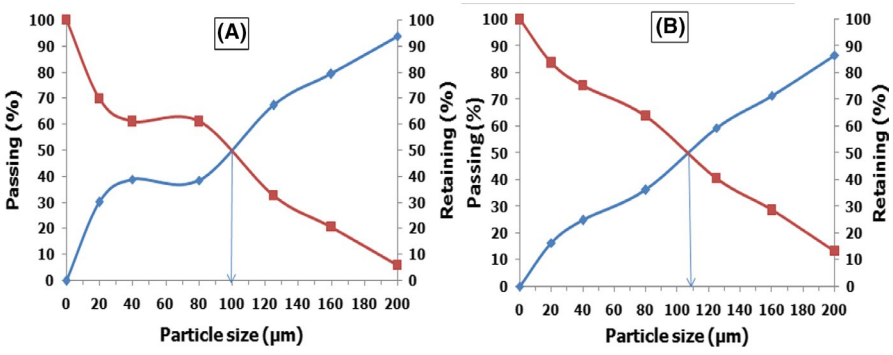

FIGURE 1 Particle size distribution curves of A: clay, B: sewage sludge ash respectively

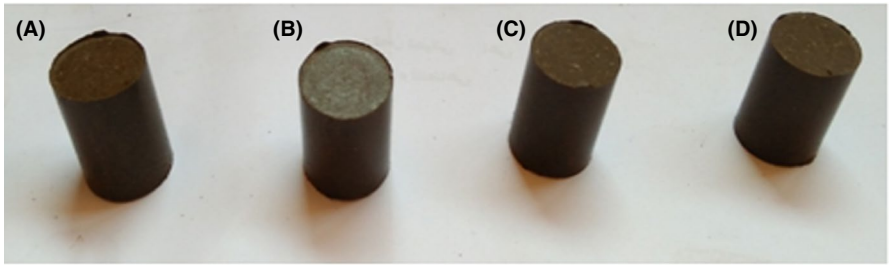

FIGURE 2 An example of the green prepared sample: A is clay/SSA (0 wt.%) and B-D are clay/SSA (20 wt.%). SSA, sewage sludge ash

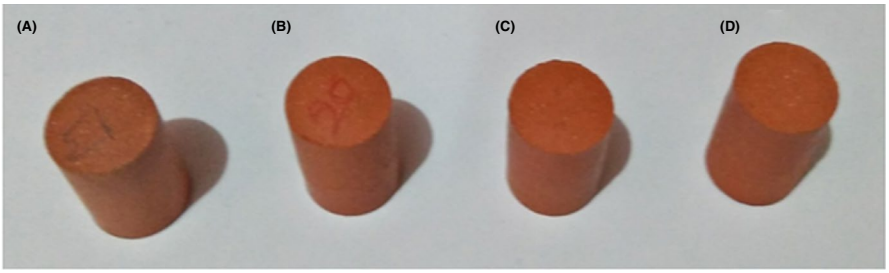

FIGURE 3 An example of the sintered samples: A is clay/SSA (0 wt.%) and B-D are clay/SSA (20 wt.%). SSA, sewage sludge ash

and linear firing shrinkage which were performed according to (ASTM C373-88 and ASTM C20-00).

Prepared samples for each concentration of clay/SSA were dried at 105°C to constant weight and the dry weight was determined (*D*) in grams. The test specimens were placed in distilled water and boiled for 2 hours. Afterwards, the test specimens were cooled to room temperature while still completely immersed in water for 24 hours. The suspended weight (*S*) of each test specimen after boiling and while suspended in water was determined. Then, the saturated weight (*W*) was determined by weighing in air.

The bulk density *B* (g/cm^3), apparent porosity *P* (%), and water absorption *A* (%) were estimated by the following equations':

$$B = D/(w-s) \tag{1}$$

$$P = \frac{W-D}{W-S} \times 100 \tag{2}$$

$$A = \frac{W-D}{D} \times 100 \tag{3}$$

The linear firing shrinkage were expressed as a percentage and calculated according to the following formula:[9]

$$\text{Linear firing shrinkage}\,(\%) = \frac{L_{\text{dried}} - L_{\text{fired}}}{L_{\text{dried}}} \times 100 \tag{4}$$

LOI was determined by measuring the mass loss of the sample between the drying and firing steps. They are expressed as a percentage and calculated according to the following formula:[9]

$$\text{Loss on ignition}\,(\%) = \frac{W_{\text{dried}} - W_{\text{fired}}}{W_{\text{dried}}} \times 100 \tag{5}$$

2.5 | Leaching test

Due to the presence of heavy metals in sewage sludge, their leachability from SSA and clay/SSA 30 wt.%) samples were determined according to the literature.[11] 500 mL of distilled water which was acidified with 1N HNO_3 to pH = 4, was added to 5 g of ground-up samples which had particle size below 125 μm. Samples prepared in this way have been stirring by a magnetic stirrer for 5 hours, and the pH of solutions throughout the process was kept constant by using 1N HNO_3. After leaching, the suspensions were centrifuged. The obtained clear solutions were filtered, and the concentration of heavy metals of the remaining elements was detected with Atomic Absorption Spectrometer (Thermo Scientific ICE 3300).[11]

3 | RESULTS AND DISCUSSION

3.1 | Characterization

3.1.1 | Chemical composition of raw clay and SSA

Table 1 shows the analysis of the chemical composition of raw clay and SSA materials. It can be noticed from the table that SiO_2 represents the high content of the clay (49.82 wt.%) followed by Al_2O_3 (2.63 wt.%) then Fe_2O_3 (10.98 wt.%) and traces of other oxides such as K_2O, Na_2O, CaO, TiO_2, and MnO. The presence of these main compounds in the raw materials of the ceramic facilitates the densification in the prepared samples since, these oxides lead to liquid phase, transformed into glass phase up on cooling and so decrease the optimum firing temperature.[11,12]

The LOI of clay is due to the vaporization of water contained in its boundaries during the ignition as well as the

TABLE 1 The chemical composition of clay raw material and SSA by XRF

Chemical constituen		SiO_2	Fe_2O_3	Al_2O_3	TiO_2	MnO	MgO	CaO	Na_2O	K_2O	P_2O_5	Cl	SO_3	LOI
(wt.%)	Clay	49.82	10.98	24.63	1.09	0.05	1.52	0.32	0.56	0.81	0.14	0.05	0.01	9.79
	SSA	10.28	7.78	2.29	0.88	0.12	0.13	8.80	0.03	0.60	1.66	0.16	5.78	61.12

Abbreviations: LOI, loss on ignition; SSA, sewage sludge ash.

organic matter in this clay.[13] For SSA, it can be seen that, only about 38 wt.% of SSA is inorganic since it showed high value for LOI (61.12 wt.%) which represents the organic matter that releases during firing.

3.1.2 | Mineralogy of the prepared samples

Figure 4 shows the XRD analysis of both clay raw material and SSA to establish the inorganic crystalline composition. The main mineral components of raw clay which were identified include quartz (SiO_2) (code: 01-074-3485) and gypsum ($CaSO_4.2H_2O$) (code: 01-074-1904), followed by kaolinite ($Al_2Si_2O_5(OH)_4$) (code: 00-001-0527) and montmorillonite ($Na_{0.3}(Al, Mg)_2Si_4O_{10}$ $(OH)_2.xH_2O$) (code: 00-058-2010) as shown in Figure 4A. For SSA, Figure 4B shows that SSA contains quartz and magnesium doped calcite ($Mg_{0.06}$ $Ca_{0.94}$) (CO_3) (code: 01-089-1305) and followed by Tamarugite (Na Al $(SO_4)_2(H_2O)_6$), (code: 01-071-2385).

Figure 5 shows the XRD pattern for clay/SSA (0, 10, 20, 30, and 40 wt.%) fired ceramic samples. It can be noticed that the Kaolinite peaks disappeared in all fired samples and the Quartz peak at ($2\Theta = 26.7°$) is more stable since it appears in all fired samples, but its intensity decreased. Also, it can be noticed that the Montmorillonite converted to Illite ($2K_2O_3{\cdot}MgO{\cdot}Al_2O_{24}{\cdot}3SiO_{12}{\cdot}2H_2O$) (code: 00-002-0050) upon firing. Also, Gypsum converted to -Anhydrite ($CaSO_4$) (code: 00-003-0162) due to the release of water molecules. Albite ($NaAlSi_3O_8$) (code: 00-001-0739) appeared and there was an increase in the anhydrite peak height as the fraction of SSA increased which confirm X-ray fluorescence (XRF) analysis. Also, the Illite decrease in higher SSA samples may be due to the interaction with the calcite of SSA.[14]

3.1.3 | Thermal analysis

Figure 6A shows the DTA and TGA curves of the clay. It can be noticed from this figure that there are four peaks, two peaks are endothermic and the other two are exothermic. The first endothermic peak at 150°C is due to the removal of physical-bound water (dehydration) from the clay with a weight loss of (3.5 wt.%) of the sample. The second endothermic change occurs with the most prevailing peak at about 550°C is due to the removal of chemical-bound water. Also, this reaction, is known as dehydroxylation, whereby part of the clay structure (hydroxyl groups) is destroyed. the XRD confirms the disappearance of the kaolinite peaks in all fired samples.[15] The weight loss of approximately 6 wt.% because of dehydroxylation is shown on the TGA curve. As for the exothermic reactions, peaks recorded at 400 and 750°C are caused by burn-off of carbonaceous organic matter, which mainly derives from plant and animal fossils in the clay samples.[15]

Figure 6B shows the DTA and TGA curves of SSA. There is a clear broad endothermic effect, beginning at 50°C and ending at 277°C and the maximum occurs at 120°C which

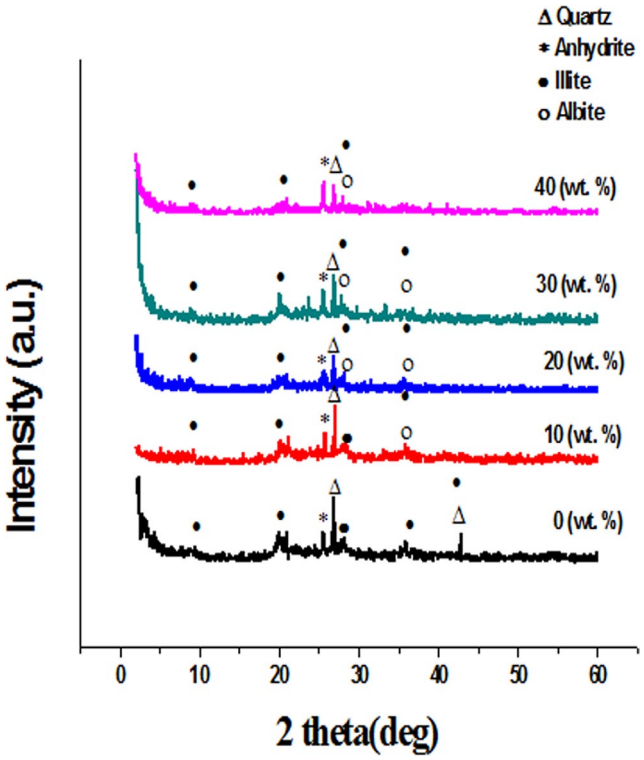

FIGURE 5 X-ray diffraction pattern for clay/sewage sludge ash (0, 10, 20, 30, and 40 wt.%)

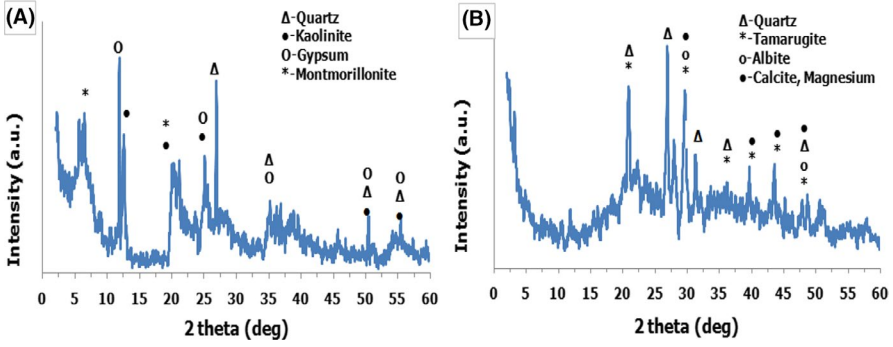

FIGURE 4 X-ray diffraction patterns of A: clay raw material and B: sewage sludge ash respectively

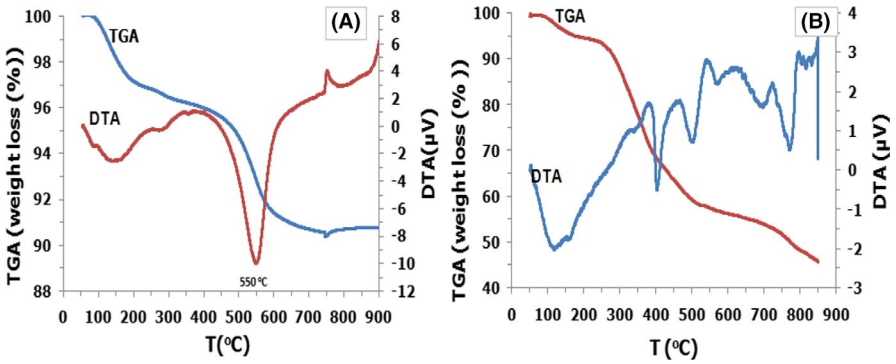

FIGURE 6 TGA and DTA for A: clay and B: sewage sludge ash respectively

is attributed to the removal of physical-bound water (dehydration). About (5.3 wt.%) of the weight was lost during this effect.[11] The endothermic effect goes to an exothermic effect with three peaks at 380, 470, and 542°C which finished around 700°C. A weight loss of about 41.9 wt.% of the initial sample is associated with this effect. In the range of 277 to 380°C, the sample has lost (16.4 wt.%) which most likely corresponds to the depolymerization reactions of biodegradable matter, and at the second step from 380 to 522°C, the weight loss of (24.1 wt.%) should be ascribed to the degradation reactions of non-biodegradable organic matter.[16] The end of this process appears in the temperature of 650-670°C and is characterized by the sudden disappearance of the exothermic. At the final step of the heating process (>700°C), a clear endothermic effect with a maximum at 771°C, during which the residual carbonaceous material and ash experienced the mass loss at slow rates.[12] Since SSA has a relatively high firing sensitivity below 650°C, it is necessary to lower the heating rate and/or to hold for some time at 650°C or higher constant temperature, in order to fully destroy the organic matter from SSA and to eliminate their impact on the sintering of ceramic samples.

The effect of SSA addition on the firing process of the samples

Figure 7A shows the TGA curves for clay/SSA (10, 20, and 30 wt.%). It can be noticed from the figure that the decomposition process can be divided into two stages. The first stage corresponds to the dehydration in the temperature range from 80-180ºC, during which; the TGA curves for different concentrations of SSA are approximately similar. As previously discussed, due to hydroxylation, the second stage became in the range of 200-600ºC instead of in the range of 400 to 600ºC with the addition of SSA to clay. This drop-in mass loss is due to the decomposition of the organic matter of SSA. The addition of SSA led to a decrease in the initial temperature of decomposition at this stage as shown in Figure 7B for DTA curves which means that SSA works as internal fuel during the combustion process of ceramic samples and the so retrieve the energy of SSA.

Kinetic analysis

The knowledge of the process which takes place during the thermal treatment of the clay is necessary to understand the sintering behavior of ceramic material and the influence of additives on the process. Coats-Red fern method was used to analyze the obtained data.[17] The obtained results with Coats-Red fern are presented in Table 2. Figure 8 shows the typical plots of $\ln(-\ln(1-\chi)/T^2)$ vs $1/T$ for clay/SSA 10 and 30 (wt.%) samples as an example in the two steps of the decomposition. The figure shows that decomposition is a first-order reaction. It can be noticed from Table 2 that the decomposition energy, E, depends on the SSA ratio and tends to decrease as this ratio increase. The organic matter in SSA seemed to facilitate the combustion process since hydroxylation shifted to a lower temperature

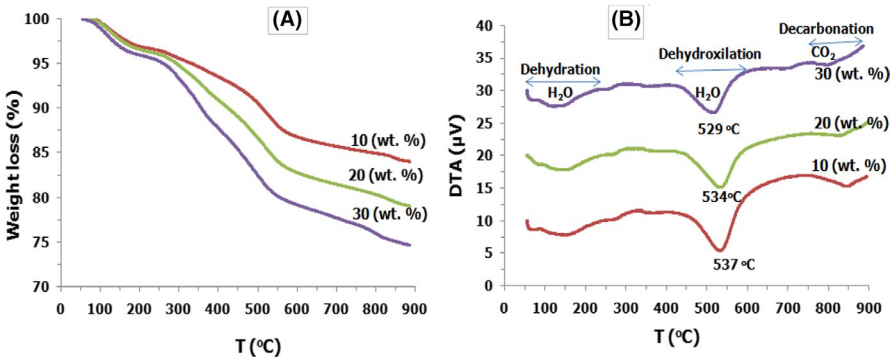

FIGURE 7 A, TGA and B: DTA for clay/sewage sludge ash (10, 20, 30 wt.%) samples

TABLE 2 Decomposition energy for clay/SSA (0, 10, 20 and 30 wt.%) (Coats-Red fern method)

SSA concentration. (wt.%)	0		10			20			30		
Range of temperature T (°C)	94-140	492-584	103-186	288-437	450-578	106-194	296-409	424-560	94-176	306-369	369-510
Decomposition energy (KJ/mole)	66.3	179.2	47.3	46.1	140.8	44.6	65.9	111.2	21.6	28.6	13.5

Abbreviation: SSA, sewage sludge ash.

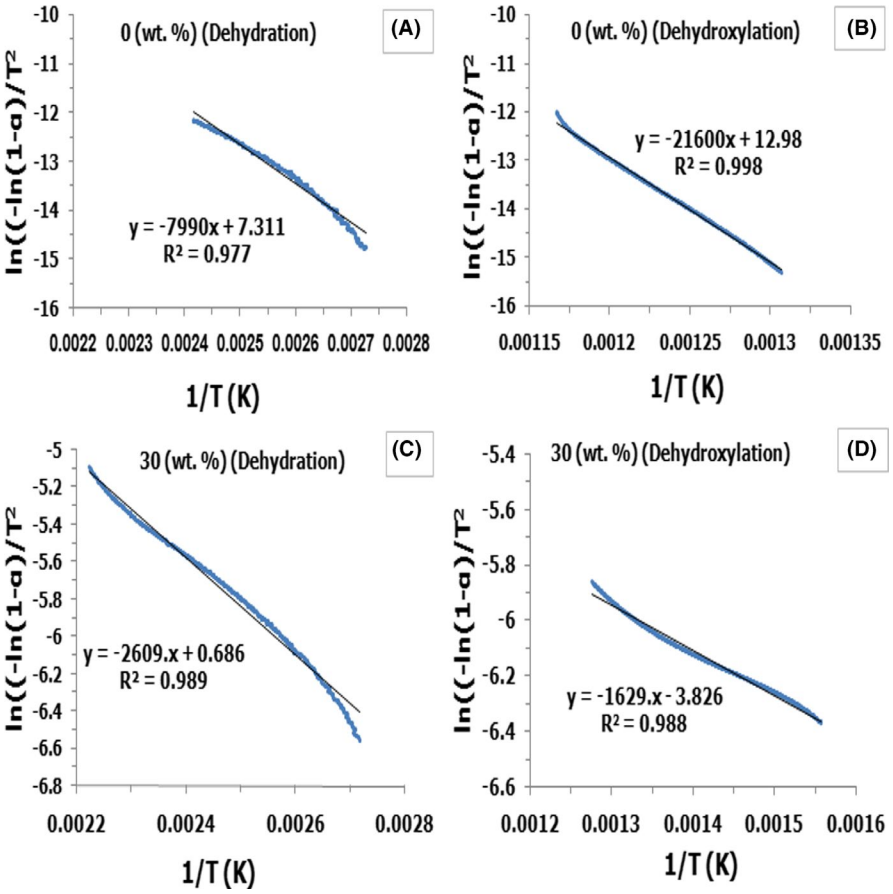

FIGURE 8 Plots of ln (−ln $(1-\chi)/T^2$) vs $1/T$: A-B for clay/SSA (10 wt.%) sample in first and second decomposition regions, respectively, and C-D clay/SSA (30 wt.%) sample in first and second decomposition regions respectively. SSA, sewage sludge ash

for higher concentration which confirmed the decrease in the consumed energy.

3.1.4 | Microstructure analysis

Figure 9 shows the SEM of the different prepared samples. It can be noticed from the figure that there are differences in the pore structure and the cracks in the prepared samples. Generally, the samples exhibited an increase in the numbers of pores and cracks with increasing SSA concentration. Also, it is noted that the nature of the samples differed, especially for the SSA ratio above (20 wt.%) since the samples became rougher as shown in Figure 9D. This is due to the increase in organic matter of SSA, which gets burning during the sintering of the samples and leaves behind many pores.[2] This is clear from EDX in Table 3 since the carbon element increases with increasing SSA ratio. Also, it is clear from Table 3 that the ratio of CaO increases and SiO_2 decreases with increasing SSA ratio in the samples which assert the XRD analysis.

3.2 | Physical properties of lightweight ceramics

3.2.1 | Bulk density and apparent porosity

Figure 10 shows the dependence of the bulk density and the apparent porosity on SSA concentration. It is clear that

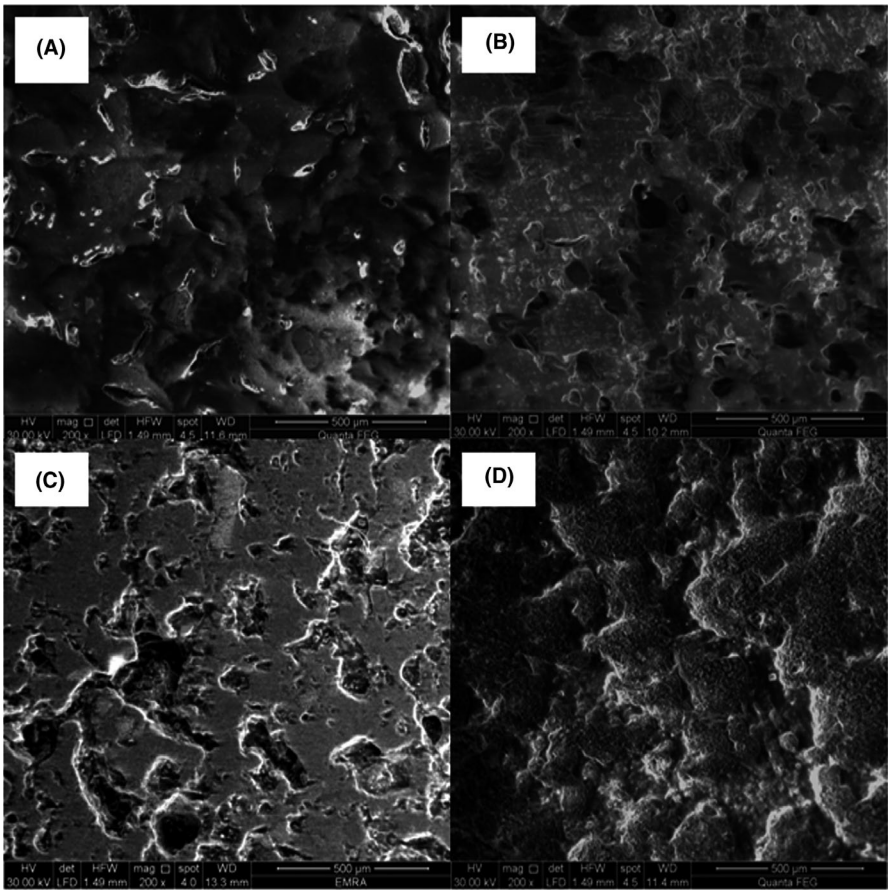

FIGURE 9 Scanning electron microscope of clay/sewage sludge ash A: (0 wt.%), B: (10 wt.%), C: (20 wt.%) and D: (30 wt.%)

the bulk density of the samples is inversely proportional to the concentration of SSA. The total organic matter in SSA is quite high as seen from thermal and XRF analyses which have been released from the ceramic products during firing leaving various pores and cracks so the porosity of the ceramic body will be increased as shown in Figure 10B and hence the density will be decreased.[2,8]

TABLE 3 EDX of clay/SSA (0, 10, 20 and 30 wt.%) samples

	SSA concentration (wt.%)			
Element	**0**	**10**	**20**	**30**
C	3.93	4.46	6.08	9.88
O	31.03	32.38	32.21	30.9
Na	1.08	0.84	0.87	1.07
Mg	1.35	1.27	1.45	1.36
Al	15.91	14.36	14.47	15.02
Si	33.57	31	30.11	23.93
Cl	0.21	0.28	0.88	0.39
K	1.44	1.28	1.35	1.25
Ca	0.55	2.42	1.82	4.06
Ti	0.98	0.93	0.88	1.05
Fe	9.95	9.11	9.88	9.47

Abbreviations: EDX, energy dispersive X-ray; SSA, sewage sludge ash.

3.2.2 | The water absorption

The water absorption is increased with increasing SSA concentrations as shown in Figure 11. During the firing of the samples, SSA makes porous structure in the ceramic body so the increase in water absorption may be due to the growth in open porosity of grains and bigger heterogeneity of the grain shape as seen from Figure 9.[11]

3.2.3 | Weight LOI and linear firing shrinkage

Figure 12 shows the weight LOI and linear firing shrinkage vs SSA concentration. It can be noticed that the increase in the SSA concentration resulted in an increase in ceramic weight LOI. As seen from the thermal and XRF analysis of SSA that about (61 wt.%) of its weight is an organic matter which releases during the firing and contributes to the increase in the loss in weight of the ceramic during the firing process.[7] Also, it can be seen that the change in the linear firing shrinkage can be attributed to the evaporation of the added water during the preparation. One can see that the change in the values of linear firing shrinkage is within the experimental error which verifies that this property is independent of SSA concentration in the mixture.[18] The quality of ceramic products can be classified according to the degree

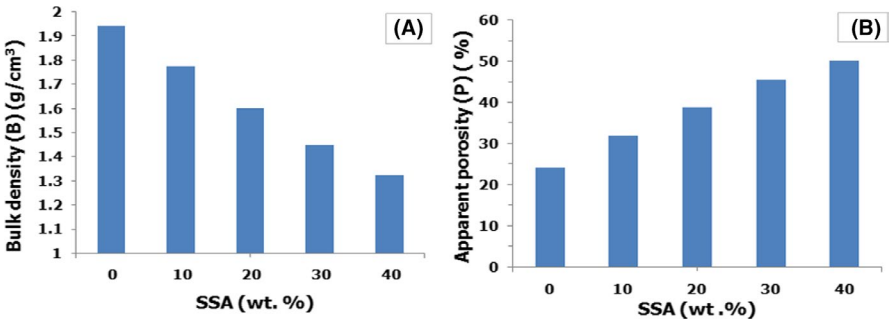

FIGURE 10 A, Bulk density and B: Apparent porosity with SSA concentration. SSA, sewage sludge ash

of firing shrinkage. Normally, for bricks, a good quality one exhibits shrinkage below 8%.[7] All of the prepared samples have shrinkage below 4%.

3.3 | Mechanical properties

3.3.1 | Compression test

Figure 13 shows the effect of SSA concentration on the compressive strength of the fired prepared samples. It can be noticed that compressive strength depends on the concentration of SSA in the samples. Compressive strength is usually affected by the porosity and the pore size so the observable reduction in strength was mainly due to the increase in porosity and consequently the decrease in density.[19] Also, one can notice that up to (30 wt.%), the ceramic samples met the Egyptian requirement for building materials.[20] Samples with greater than (30 wt.%) of SSA addition are not suitable for use since they are fragile and easily deform.

3.4 | Leachability test

Leachability measurements of elements in water extracts showed that the presence of toxic metals in SSA is relatively

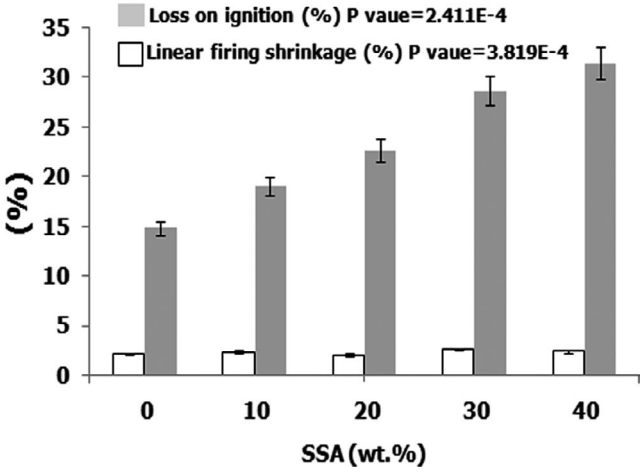

FIGURE 12 The weight loss on ignition and the linear firing shrinkage vs SSA concentration. SSA, sewage sludge ash

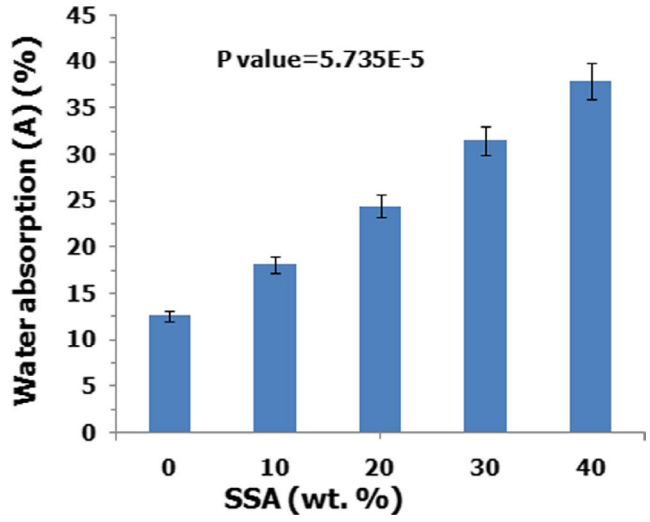

FIGURE 11 Water absorption with SSA concentration. SSA, sewage sludge ash

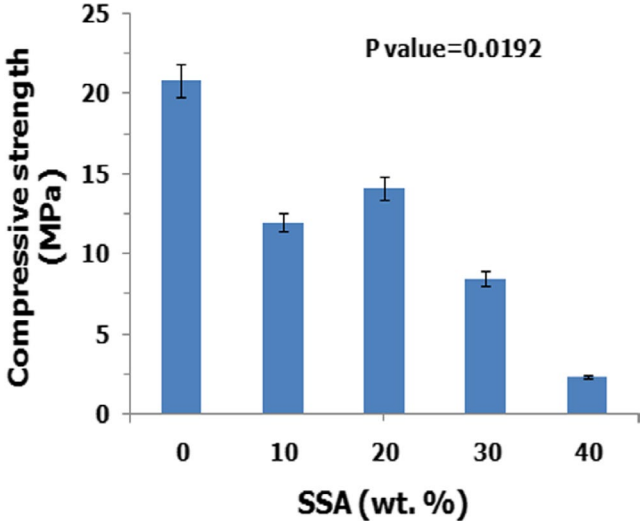

FIGURE 13 The effect of SSA concentration on the compressive strength of the fired samples. SSA, sewage sludge ash

TABLE 4 Concentrations of heavy metals in SSA and clay/SSA (30 wt.%) samples

Heavy metal (mg/L)	SSA (mg/L)	Clay/SSA 30 wt.% (mg/L)	Standard
Cu	0.081	0.009	2
Cd	0.023	Nd	0.003
Fe	0.415	Nd	0.3
Zn	3.454	0.637	3
Cr	Nd	Nd	0.05
Mn	1.150	0.203	0.1
Pb	Nd	Nd	0.01
Ni	0.11	0.124	0.02

Abbreviations: Nd: not detected; SSA, sewage sludge ash.

higher than the threshold values as prescribed in (Egyptian standard specification of drinking water 2007) as shown in Table 4. On the other hand, clay/SSA (30 wt.%) sample has shown dropping in the presence of those metals. This means that the metal elements solidified in the sintered samples and are harmless to the environment.[21]

4 | CONCLUSIONS

SSA was used with clay to obtain lightweight ceramics. The chemical composition of SSA was close to clay. The densities of the fired samples varied between 1.94 and 1.32 g/cm^3, which means a decrease in 38% compared to the density of the sample without SSA. The results showed that SSA enhances the combustion process of the samples. Small shrinkage occurred in the samples due to dehydration. Water absorption and apparent porosity were increased with the increase in SSA concentration. The porosity and shape of pores have a noticeable effect on the mechanical strength. The compressive strength of the samples decreased with SSA concentration but, it is still higher than the Egyptian standard strength values. It can be concluded from the above results that lightweight ceramics with acceptable compressive strength were obtained with a reduction in the consumed energy in the firing process.

ACKNOWLEDGMENT

The authors thank the Water Treatment Plant in Benha (Egypt) for their help in providing SSA for this research. In addition, the authors thank the staff members of the physics department faculty of science at Benha University, Egypt for accessing their laboratories.

ORCID

Asmaa A. Negm https://orcid.org/0000-0002-0450-6805

Tarek Y. Elrasasi https://orcid.org/0000-0002-2133-7724

REFERENCES

1. Smol M, Kulczycka J, Henclik A, Gorazda K, Wzorek Z. The possible use of sewage sludge ash (SSA) in the construction industry as a way towards a circular economy. J Clean Prod. 2015;95:45–54. https://doi.org/10.1016/j.jclepro.2015.02.051.
2. Wang X, Jin Y, Wang Z, Mahar RB, Nie Y. A research on sintering characteristics and mechanisms of dried sewage sludge. J Hazard Mater. 2008;160:489–94. https://doi.org/10.1016/j.jhazmat.2008.03.054.
3. Zhou J, Li T, Zhang Q, Wang Y, Shu Z. Direct-utilization of sewage sludge to prepare split tiles. Ceram Int. 2013;39(8):9179–86. https://doi.org/10.1016/j.ceramint.2013.05.019.
4. Wang X, Jin Y, Wang Z, Nie Y, Huang Q, Wang Q. Development of lightweight aggregate from dry sewage sludge and coal ash. Waste Manag. 2009;29(4):1330–5. https://doi.org/10.1016/j.wasman.2008.09.006.
5. Morais LC, Dweck J, Campos V, Büchler PM. Characterization of sewage sludge ashes to be used as a ceramic raw material. Chem Eng Trans. 2009;17:1813–8.
6. Zhang YM, Jia LT, Mei H, Cui Q, Zhang PG, Sun ZM. Fabrication, microstructure and properties of bricks fired from lake sediment, cinder and sewage sludge. Constr Build Mater. 2016;121:154–60. https://doi.org/10.1016/j.conbuildmat.2016.05.155.
7. Benlalla A, Elmoussaouiti M, Dahhou M, Assa M. Utilization of water treatment plant sludge in structural ceramics bricks. Appl Clay Sci. 2015;118:171–7. https://doi.org/10.1016/j.clay.2015.09.012.
8. Kizinievič O, Žurauskiene R, Kizinievič V, Žurauskas R. Utilisation of sludge waste from water treatment for ceramic products. Constr Build Mater. 2013;41:464–73. https://doi.org/10.1016/j.conbuildmat.2012.12.041.
9. Bories C, Borredon M, Vedrenne E, Vilarem G. Development of eco-friendly porous fi red clay bricks using pore-forming agents: a review. J Environ Manage. 2014;143:186–96. https://doi.org/10.1016/j.jenvman.2014.05.006.
10. Muñoz Velasco P, Morales Ortíz MP, Mendívil Giró MA, Muñoz VL. Fired clay bricks manufactured by adding wastes as sustainable construction material—a review. Constr Build Mater. 2014;63:97–107. https://doi.org/10.1016/j.conbuildmat.2014.03.045.
11. Franus M, Barnat-Hunek D, Wdowin M. Utilization of sewage sludge in the manufacture of lightweight aggregate. Environ Monit Assess. 2016;188(1):1–13. https://doi.org/10.1007/s10661-015-5010-8.
12. Escalera E, Tegman R, Antti ML, Odén M. High temperature phase evolution of Bolivian kaolinitic-illitic clays heated to 1250°C. Appl Clay Sci. 2014;101:100–5. https://doi.org/10.1016/j.clay.2014.07.024.
13. Johari I. Chemical and physical properties of fired-clay brick at different type of rice husk ash. Int Conf Environ. 2011;8:171–4.
14. Coletti C, Cultrone G, Maritan L, Mazzoli C. How to face the new industrial challenge of compatible, sustainable brick production: study of various types of commercially available bricks. Appl Clay Sci. 2016;124–125:219–26. https://doi.org/10.1016/j.clay.2016.02.014.
15. Liew AG, Idris A, Wong CHK, Samad AA, Noor MJMM, Baki AM. Incorporation of sewage sludge in clay brick and its

characterization. Waste Manag Res. 2004;22(4):226–33. https://doi.org/10.1177/0734242X04044989.
16. Strezov V, Evans TJ, Kan T, Strezov V, Evans T. Thermochemical behaviour of sewage sludge during its slow pyrolysis thermochemical behaviour of sewage sludge during its slow pyrolysis. Int J Adv Mech Civ Eng. 2015;2:64–7.
17. Apaydin-varol E, Polat S, Putun AE. Pyrolysis kinetics and thermal decomposition behavior of polycarponate—a TGA-FTIR study. Therm Sci. 2014;18(3):833–42. https://doi.org/10.2298/TSCI1403833A.
18. Jordán MM, Almendro-candel MB, Romero M, Rincón JM. Application of sewage sludge in the manufacturing of ceramic tile bodies. Appl Clay Sci. 2005;30:219–24. https://doi.org/10.1016/j.clay.2005.05.001.
19. Aeslina K, Kadir A, Onn H. Recycling cigarette butts in lightweight fired clay bricks. Constr Mater. 2011;164(5):219–29. https://doi.org/10.1680/coma.900013.
20. Hegazy B-D, Fouad HA, Hassanain AM. Incorporation of water sludge, silica fume, and rice husk ash in brick making. Adv Environ Res. 2012;1(1):83–96.
21. Qi Y, Yue Q, Han S, Yue M, Gao B, Yu H, et al. Preparation and mechanism of ultra-lightweight ceramics produced from sewage sludge. J Hazard Mater. 2010;176:76–84. https://doi.org/10.1016/j.jhazmat.2009.11.001.

How to cite this article: Negm AA, Elrasasi TY, Khoder HA, Metawe FM, El-Mansy MK. Preparation, characterization, and physical properties of lightweight ceramics by using sewage sludge ash. *Int J Appl Ceram Technol*. 2020;00:1–10. https://doi.org/10.1111/ijac.13456